Charge ordered metal and pressure-induced superconductivity in the two-dimensional organic conductor β''-$(DODHT)_2PF_6$

2008 J. Phys.: Condens. Matter 20 125205

(http://iopscience.iop.org/0953-8984/20/12/125205)

J. Phys.: Condens. Matter **20** (2008) 125205 (6pp) doi:10.1088/0953-8984/20/12/125205

Charge ordered metal and pressure-induced superconductivity in the two-dimensional organic conductor β''-$(DODHT)_2PF_6$

Akito Kobayashi[1,2], Yoshikazu Suzumura[2], Momoka Higa[3], Ryusuke Kondo[3], Seiichi Kagoshima[3] and Hiroyuki Nishikawa[4]

[1] Institute for Advanced Research, Nagoya University, Japan
[2] Department of Physics, Nagoya University, Japan
[3] Department of Basic Science, University of Tokyo, Japan
[4] Department of Chemistry, University of Tsukuba, Japan

E-mail: akito@slab.phys.nagoya-u.ac.jp

Received 15 October 2007, in final form 28 January 2008
Published 25 February 2008
Online at stacks.iop.org/JPhysCM/20/125205

Abstract

The superconductivity in a quasi-two-dimensional organic conductor, β''-$(DODHT)_2PF_6$ salt, which is expected to appear after the melting of a charge ordering (CO) state, has been examined using an extended Hubbard model with anisotropy for both the transfer energies and the nearest-neighbor repulsive interactions between the DODHT molecules. The fluctuation is treated by the random phase approximation based on mean-field calculation of the CO. When pressure is applied, an insulating state with CO (COI) changes into a metallic state with weakened CO (COM) at an intermediate pressure, and a normal state without CO emerges at higher pressures. For the COM state at intermediate pressure, the COI state and the normal state also exist as metastable states, and their free energies are nearly the same within a narrow energy range of 10^{-3} eV. Thus these three states may coexist with each other by forming a phase separation at finite temperature. We find that the spin fluctuation around such a mean-field COM state gives rise to a superconducting state with a full gap. Further, we suggest that d-wave superconductivity mediated by the charge fluctuation occurs in the normal state with a quasi-one-dimensional Fermi surface when the nearest-neighbor interaction becomes as large as the *on-site* interaction.

1. Introduction

There are hundreds of quasi-two-dimensional organic conductors which exhibit superconductivity located in the vicinity of other ordered phases at low temperatures [1, 2]. Among them, the β''-$(DODHT)_2PF_6$ salt exhibits a superconducting (SC) state when charge ordering (CO) disappears upon the application of pressure [3–5]. In figure 1(a), a phase diagram is shown on the plane of pressure and temperature where the onset temperatures for the insulator (squares) and for superconductivity (triangles) are obtained from resistivity measurements [5]. The transfer integrals, which are estimated from the crystal structure analysis, exhibit a large Fermi surface, although the increase of resistivity with decreasing temperature suggests a semiconductor-like behavior for low pressures ($P < 11$ kbar). At ambient pressure, a steep increase of resistivity at $T = T_I = 250$ K (squares) is followed by a stripe charge ordering (CO) along the p–q direction (see figure 1(b)), which exists in the low temperature phase ($T < T_I$). With increasing pressure, T_I decreases and the salt exhibits a rather metallic behavior at high pressures ($P > 11$ kbar), in the sense that the increase in resistivity is strongly reduced at temperatures lower than T_I' (circles). At these high pressures, the distinct metal–insulator transition disappears, and superconductivity with a critical temperature of $T_c \sim 2.3$ K emerges for $13 < P < 18$ kbar. It remains unclear if the superconductivity

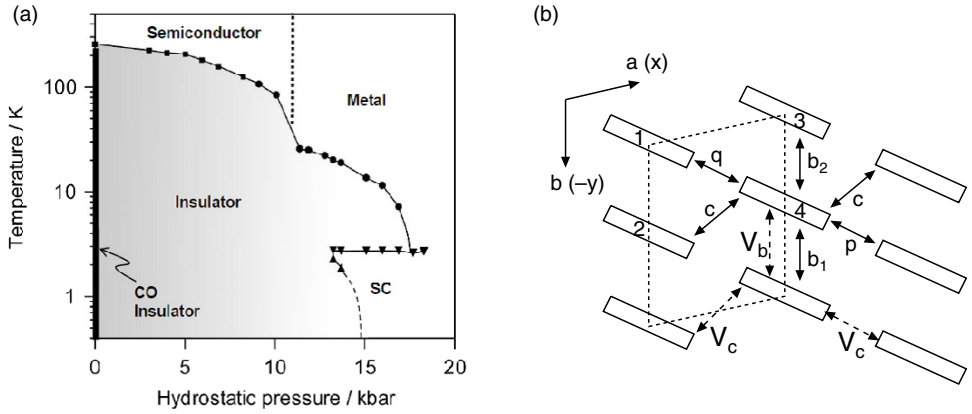

Figure 1. (a) Phase diagram of β''-(DODHT)$_2$PF$_6$ salt on the plane of hydrostatic pressure and temperature [5]. The states of semiconductor, insulator, superconductor (SC) and metal are obtained from resistivity measurements. (b) The model for the electronic system of β''-(DODHT)$_2$PF$_6$ salt. The unit cell enclosed by the dotted line consists of two DODHT molecules (sites 1 and 2) with five transfer energies and two kinds of nearest-neighbor repulsive interactions, V_b and V_c. The indices of sites 1, 2, 3, and 4 correspond to the extended unit cell of the superlattice in the stripe CO along the p–q direction.

is compatible with the CO state. Further we note that the electronic state in the 'semiconductor-like' region above T_I is similar to the weak increase in the resistivity below T_I'.

Theoretical work on the CO state has been performed using the extended Hubbard models for organic conductors [6–10]. It is shown that the anisotropic repulsive interaction between the nearest-neighbor sites plays an important role in the formation of the stripe CO. The mechanisms of the superconductivity related to the CO state have been suggested for several salts. It is maintained that superconductivity in the presence of CO [11] is induced by spin fluctuation in the charge ordered metal (COM) for α-(BEDT-TTF)$_2$I$_3$. This COM is interpreted as a self-doped Heisenberg chain in the stripe CO weakened by the uniaxial pressure [10]. COMs have also been investigated in the square lattice model [12] and in a model for θ-(BEDT-TTF)$_2$X [13]. These states are induced by the intersite Coulomb interaction V, and are located between an insulator with CO and the normal (homogeneous) metal. Organic superconductors which occur in the normal state in the vicinity of the CO have also been investigated [14–19, 13, 20], showing that the mechanism may be ascribed to charge fluctuation. However, for SC in the present case, which occurs in the metallic state at high pressures, the resistivity increases in a narrow region of temperature above T_c, indicating that the metallic state coexists with the CO state or the 'semiconductor-like' state. Thus it is not clear which type of pairing mechanism, i.e. spin fluctuation or charge fluctuation, gives rise to the SC state in the present salt.

In the present paper we investigate those unique electronic states for the CO and the SC states described above by applying the random phase approximation to an extended Hubbard model, where the CO is treated within mean-field theory. The transfer integrals in the model are taken from the data of the x-ray experiment of [5] in order to apply the actual electronic state of β''-(DODHT)$_2$PF$_6$ salt. The purpose of the present calculation is to demonstrate explicitly the following facts. A COM with weakened CO exists in the intermediate pressure region between the insulating state with the stripe CO and the normal metallic state. The free energies for such an intermediate region are almost degenerate within a narrow energy range of 10^{-3} eV, and then metastable states are expected to coexist at finite temperature. The spin fluctuation is enhanced in the COM and induces superconductivity with a full gap, which is favorable as a pairing mechanism as pointed out by Kuroki and Arita [21]. On the other hand, the superconductivity mediated by the charge fluctuation occurs in the normal state.

Table 1. The transfer energies (eV) of the β''-(DODHT)$_2$PF$_6$ for $P = 0$, 7.5 and 19 kbar, respectively.

P	$b1$	$b2$	c	p	q
0	0.0219	0.0096	0.1099	0.1086	0.0814
7.5	0.0204	0.0181	0.1177	0.1249	0.0850
19	0.0225	0.0495	0.1289	0.1732	0.1425

2. Model and formulation

The basic model for the 2D conducting plane of the β''-(DODHT)$_2$PF$_6$ salt is shown in figure 1(b). The dotted parallelogram denotes the unit cell with two DODHT molecules where sites 1 and 2 are equivalent to sites 3 and 4, respectively, for the normal state. The transfer energies b_1, b_2, c, p and q are calculated by the extended Hückel method on the basis of the data from the x-ray experiment [5]. The pressure (P) dependence of the transfer integrals is estimated using the linear interpolation formula for $P = 0$, 7.5 and 19 kbar, listed in table 1 [22].

There are three electrons in the two molecules due to the 3/4-filled band. These transfer energies in the absence of interactions give a large one-dimensional-like Fermi surface and a small two-dimensional like hole pocket [5]. In order to explain the stripe CO along the p–q direction, we consider the anisotropic nearest-neighbor Coulomb interactions V_b and V_c in addition to the on-site Coulomb interaction U. In

our calculation, the x-axis (the y-axis) corresponds to the a-direction (the b-direction).

The extended Hubbard model for β''-(DODHT)$_2$PF$_6$ salt is given by

$$H = \sum_{\langle i\alpha:j\beta\rangle,\sigma} (t_{i\alpha;j\beta}\, a^{\dagger}_{i\alpha\sigma} a_{j\beta\sigma} + \text{H.c.}) + \sum_{i\alpha} U\, a^{\dagger}_{i\alpha\uparrow} a^{\dagger}_{i\alpha\downarrow} a_{i\alpha\downarrow} a_{i\alpha\uparrow} + \sum_{\langle i\alpha:j\beta\rangle,\sigma,\sigma'} V_{\alpha\beta}\, a^{\dagger}_{i\alpha\sigma} a^{\dagger}_{j\beta\sigma'} a_{j\beta\sigma'} a_{i\alpha\sigma}, \quad (1)$$

where $i, j(=1, \ldots N_L)$ denote site indices of the unit cell forming a 2D square lattice. The indices $\alpha, \beta = 1, 2$ are for molecules in the unit cell, and $\alpha, \beta = 1, 2, 3, 4$, are for those in the extended unit cell of the superlattice with the stripe CO state. In the first term, $a^{\dagger}_{i\alpha\sigma}$ denotes a creation operator with spin $\sigma(= \uparrow, \downarrow)$ and $t_{i\alpha;j\beta}$ is the transfer energy between the (i, α) site and the (j, β) site. The second and third terms of equation (1) denote interactions for the on-site repulsion and the nearest-neighbor repulsion, respectively. For nearest-neighbor repulsion, we distinguish $V_{\rm b}$ from $V_{\rm c}$ (see figure 1(b)), i.e. anisotropic interactions. There is a reasonable parameter range of $V_{\rm b}$ and $V_{\rm c}$, which leads to a CO pattern that is consistent with the experiment. We take $V_{\rm b} = 0.45$ and $V_{\rm c} = 0.2$ with $U = 0.5$ in order to demonstrate the stripe CO along the p–q direction.

The CO state is investigated using the mean-field (MF) theory, where the MF Hamiltonian is given by

$$H_{\rm MF} = \sum_{\mathbf{k}\alpha\beta\sigma} \tilde{\epsilon}_{\alpha\beta\sigma}(\mathbf{k})\, a^{\dagger}_{\mathbf{k}\alpha\sigma} a_{\mathbf{k}\beta\sigma} - \left(\sum_{\alpha} U_{\alpha} \langle n_{\alpha\uparrow}\rangle \langle n_{\alpha\downarrow}\rangle + \sum_{\langle\alpha,\beta\rangle\sigma,\sigma'} V_{\alpha\beta} \langle n_{\alpha\sigma}\rangle \langle n_{\beta\sigma'}\rangle \right), \quad (2)$$

$$\tilde{\epsilon}_{\alpha\beta\sigma}(\mathbf{k}) = \delta_{\alpha\beta}\left[U_{\alpha}\langle n_{\alpha\bar{\sigma}}\rangle + \sum_{\beta'\sigma'} V_{\alpha\beta'} \langle n_{\beta'\sigma'}\rangle \right] + \epsilon_{\alpha\beta}(\mathbf{k}), \quad (3)$$

where $\bar{\sigma} = -\sigma$. The matrix element, $\epsilon_{\alpha\beta}(\mathbf{k})$ is obtained in a similar way to [23] as

$$\epsilon_{\alpha\beta}(\mathbf{k}) = \sum_{\boldsymbol{\delta}} t_{\alpha\beta} \mathrm{e}^{\mathrm{i}\mathbf{k}\cdot\boldsymbol{\delta}}. \quad (4)$$

The Hamiltonian (2) is diagonalized by

$$\sum_{\beta=1} \tilde{\epsilon}_{\alpha\beta\sigma}(\mathbf{k})\, d_{\beta r\sigma}(\mathbf{k}) = \xi_{r\sigma}(\mathbf{k}) d_{\alpha r\sigma}(\mathbf{k}), \quad (5)$$

where $\xi_{r\sigma}$ is the eigenvalue with a descending order with respect to r. On the basis of the mean-field Hamiltonian, we obtain the number of electrons on the α-site with spin σ, $n_{\alpha\sigma} = \langle a^{\dagger}_{i\alpha\sigma} a_{i\alpha\sigma}\rangle$, the diagonalized band dispersion $\xi_{r\sigma}(\mathbf{k})$, and the corresponding eigenvector $d_{\alpha r\sigma}(\mathbf{k})$ $(r = 1, 2, 3, 4)$ [23].

In order to investigate the pairing interaction, we calculate susceptibilities, $\hat{X}$, defined by

$$\left(\hat{X}^{0}_{\sigma\sigma'}(\mathbf{q}, \mathrm{i}\omega_m)\right)_{\alpha\beta} = -T N_L^{-1} \sum_{\mathbf{k}\mathbf{k}'} \int_0^{1/T} \mathrm{d}\tau \mathrm{e}^{\mathrm{i}\omega_m\tau} \times \left\langle T_{\tau}\left(a^{\dagger}_{\mathbf{k}+\mathbf{q}\alpha\sigma}(\tau) a_{\mathbf{k}\alpha\sigma'}(\tau) a^{\dagger}_{\mathbf{k}'\beta\sigma'}(0) a_{\mathbf{k}'+\mathbf{q}\beta\sigma}(0)\right)\right\rangle, \quad (6)$$

which denotes the matrix element of the site representation and depends on spins σ and σ'. The quantities ω_m and τ are the Matsubara frequency for a boson and the imaginary time, respectively. $a_{i\alpha\sigma} = N_L^{-1/2} \sum_{\mathbf{k}} \mathrm{e}^{\mathrm{i}\mathbf{k}\cdot\mathbf{r}_i} a_{\mathbf{k}\alpha\sigma}$. The irreducible susceptibility $\hat{X}^{0}_{\sigma\sigma'}$ corresponding to equation (6) without fluctuation is written as

$$\left(\hat{X}^{0}_{\sigma\sigma'}(\mathbf{q}, \mathrm{i}\omega_m)\right)_{\alpha\beta} = -T N_L^{-1} \sum_{\mathbf{k}n} \left[G^{0}_{\alpha\beta\sigma}(\mathbf{k}+\mathbf{q}, \mathrm{i}\omega_m + \mathrm{i}\epsilon_n)\, G^{0}_{\beta\alpha\sigma'}(\mathbf{k}, \mathrm{i}\epsilon_n)\right], \quad (7)$$

where ϵ_n denotes the Matsubara frequency for a fermion and the single-particle Green function is given by $G^{0}_{\alpha\beta\sigma}(\mathbf{k}, \mathrm{i}\epsilon_n) = \sum_r d_{\alpha r\sigma}(\mathbf{k})\, d^{*}_{\beta r\sigma}(\mathbf{k})/(\mathrm{i}\epsilon_n - \xi_{r\sigma}(\mathbf{k}) + \mu)$, with μ being the chemical potential.

Next, by treating the fluctuations in terms of RPA, equation (6) is calculated as $\hat{X}_{\sigma\sigma} = (\hat{A}_{\sigma} - \hat{B}_{\sigma}\hat{A}^{-1}_{\bar{\sigma}}\hat{B}_{\bar{\sigma}})^{-1}\hat{X}^{0}_{\sigma\sigma}$ and $\hat{X}_{\sigma\bar{\sigma}} = (\hat{A}_{\sigma} - \hat{B}_{\sigma}\hat{A}^{-1}_{\bar{\sigma}}\hat{B}_{\bar{\sigma}})^{-1}\hat{B}_{\sigma}\hat{A}^{-1}_{\bar{\sigma}}\hat{X}^{0}_{\bar{\sigma}\bar{\sigma}}$,where $\hat{A}_{\sigma} = 1 + \hat{X}^{0}_{\sigma\sigma}\hat{V}$ and $\hat{B}_{\sigma} = \hat{X}^{0}_{\sigma\sigma}(\hat{U} + \hat{V})$. Then we obtain the pairing interaction $\hat{P}$, which consists of the spin and the charge fluctuations. For the singlet pairing SC state, there are two kinds of interactions, $P^{B}_{\alpha\sigma:\beta\bar{\sigma}}$ and $P^{L}_{\alpha\sigma:\beta\bar{\sigma}}$, with the scattering described by the bubble term and the ladder term, respectively. In the former scattering, the site indices α and β of the electrons are retained while their indices are exchanged in the latter process. These interactions are obtained as $P^{B}_{\alpha\sigma:\beta\bar{\sigma}} = \hat{U} + \hat{V} - \sum_{\sigma_1\sigma_2} \hat{I}_{\sigma\sigma_1}\hat{X}_{\sigma_1\sigma_2}\hat{I}_{\sigma_2\bar{\sigma}}$, and $P^{L}_{\alpha\sigma:\beta\bar{\sigma}} = (\hat{U}(\hat{I} - \hat{X}^{0}_{\sigma\bar{\sigma}}\hat{U})^{-1}\hat{X}^{0}_{\sigma\bar{\sigma}}\hat{U})_{\alpha\beta}$, where $(\hat{U})_{\alpha\beta} = U\delta_{\alpha\beta}$, $(\hat{V})_{\alpha\beta} = V_{\alpha\beta}(\mathbf{q}) = 2^{-1}\sum_{\boldsymbol{\delta}} V_{\alpha\beta}\, \mathrm{e}^{-\mathrm{i}\mathbf{q}\cdot\boldsymbol{\delta}}$ and $\hat{I}_{\sigma_1\sigma_2} = \hat{U}\delta_{\sigma_1\bar{\sigma}_2} + \hat{V}$. For the triplet pairing SC state, the pairing interaction is given by $P^{T}_{\alpha\sigma:\beta\sigma} = \hat{V} - (\hat{U} + \hat{V})\hat{X}_{\bar{\sigma}\bar{\sigma}}(\hat{U} + \hat{V}) - (\hat{U} + \hat{V})\hat{X}_{\bar{\sigma}\sigma}\hat{V} - \hat{V}\hat{X}_{\sigma\bar{\sigma}}(\hat{U} + \hat{V}) - \hat{V}\hat{X}_{\sigma\sigma}\hat{V}$.

From $P^{B}_{\alpha\sigma:\beta\bar{\sigma}}$ and $P^{L}_{\alpha\sigma:\beta\bar{\sigma}}$, the linearized gap equation for the singlet SC state is written as

$$\lambda\Sigma^{a}_{\alpha\sigma:\beta\bar{\sigma}}(\mathbf{k}) = -\frac{T}{N_L}\sum_{\mathbf{k}'n'\alpha'\beta'\eta\eta'} \times \left[(P^{B}_{\alpha\sigma:\beta\bar{\sigma}}(\mathbf{k}-\mathbf{k}')\delta_{\alpha\eta}\delta_{\beta\eta'} + P^{L}_{\alpha\sigma:\beta\bar{\sigma}}(\mathbf{k}+\mathbf{k}')\delta_{\alpha\eta'}\delta_{\beta\eta}) \times G^{0}_{\eta\alpha'\sigma}(\mathbf{k}', \mathrm{i}\epsilon_{n'})\, G^{0}_{\eta'\beta'\bar{\sigma}}(-\mathbf{k}', -\mathrm{i}\epsilon_{n'})\Sigma^{a}_{\alpha'\sigma:\beta'\bar{\sigma}}(\mathbf{k}')\right]. \quad (8)$$

From $P^{T}_{\alpha\sigma:\beta\sigma}$, the linearized gap equation for the triplet SC state is written as

$$\lambda\Sigma^{a}_{\alpha\sigma:\beta\sigma}(\mathbf{k}) = -\frac{T}{N_L}\sum_{\mathbf{k}'n'\alpha'\beta'} P^{T}_{\alpha\sigma:\beta\sigma}(\mathbf{k}-\mathbf{k}') \times G^{0}_{\alpha\alpha'\sigma}(\mathbf{k}', \mathrm{i}\epsilon_{n'})\, G^{0}_{\beta\beta'\sigma}(-\mathbf{k}', -\mathrm{i}\epsilon_{n'})\Sigma^{a}_{\alpha'\sigma:\beta'\sigma}(\mathbf{k}'). \quad (9)$$

The SC transition temperature $T_{\rm c}$ is given by the condition $\lambda = 1$, and the properties of the SC state are obtained from the anomalous self-energy $\Sigma^{a}_{\alpha\beta}(\mathbf{k})$. In equation (9), the frequency dependence of $\Sigma^{a}_{\alpha\beta}(\mathbf{k})$ is neglected because it is expected to be valid for the weak coupling case [16].

We note that the pairing interactions in equations (8) and (9) can be re-expressed in the following simple forms for the nonmagnetic phase which are obtained by the mean-field calculation in the next section. The singlet pairing interaction

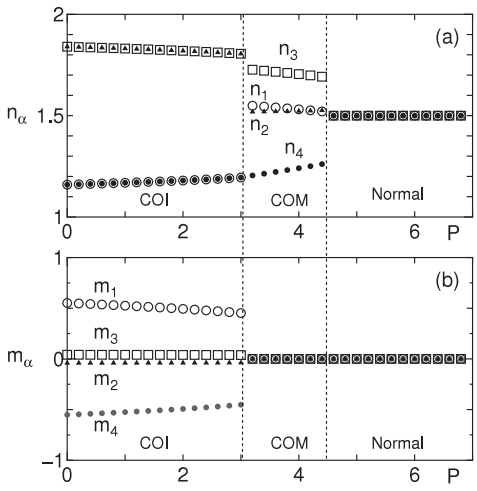

Figure 2. The pressure (P kbar) dependence of the electron number n_α and the magnetic moment m_α for $T = 0.05$, where the symbols, open circle, closed circle, open square and closed triangle denote $\alpha = 1, 2, 3$ and 4, respectively, in the extended unit cell of the superlattice.

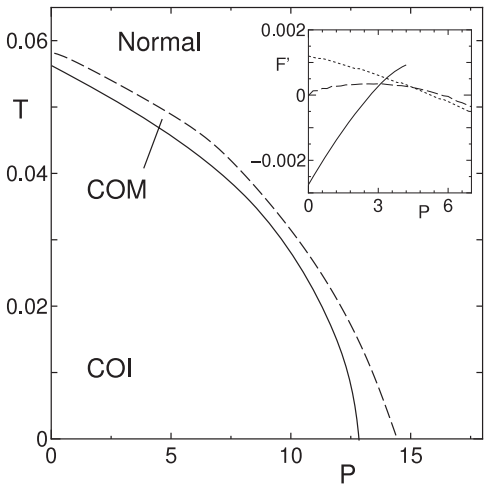

Figure 3. The pressure–temperature phase diagram consists of COI, COM and normal states. The inset shows free energies of the COI (solid line), COM (dashed line) and normal (dotted line) states where the free energy of the COM is taken as the origin. Coexistence is expected for these three states in the intermediate region ($3 < P < 4.4$), and for the COM state and the normal state in the high pressure region ($P > 4.4$).

is divided into a spin-fluctuation term, $P^{\rm s}$, and a charge-fluctuation term, $P^{\rm c}$ as:

$$P_{\alpha\sigma:\beta\bar{\sigma}} = P^{B}_{\alpha\sigma:\beta\bar{\sigma}} + P^{L}_{\alpha\sigma:\beta\bar{\sigma}} = P^{\rm s}_{\alpha\sigma:\beta\bar{\sigma}} + P^{\rm c}_{\alpha\sigma:\beta\bar{\sigma}}, \tag{10}$$

where

$$P^{\rm s}_{\alpha\sigma:\beta\bar{\sigma}} = \hat{U} + \tfrac{3}{2}\hat{U}\hat{X}^{\rm s}\hat{U}, \tag{11}$$

$$P^{\rm c}_{\alpha\sigma:\beta\bar{\sigma}} = \hat{V} - \tfrac{1}{2}(\hat{U} + 2\hat{V})\hat{X}^{\rm c}(\hat{U} + 2\hat{V}), \tag{12}$$

and $\hat{X}^{\rm s}$ and $\hat{X}^{\rm c}$ are the spin susceptibility and the charge susceptibility, respectively, given by

$$\hat{X}^{\rm s} = \tfrac{1}{2}\hat{X}_{\uparrow\uparrow} - \hat{X}_{\uparrow\downarrow} - \hat{X}_{\downarrow\uparrow} + \hat{X}_{\downarrow\downarrow}, \tag{13}$$

$$\hat{X}^{\rm c} = \tfrac{1}{2}\hat{X}_{\uparrow\uparrow} + \hat{X}_{\uparrow\downarrow} + \hat{X}_{\downarrow\uparrow} + \hat{X}_{\downarrow\downarrow}. \tag{14}$$

The triplet pairing interaction is given by

$$P^{T}\alpha\sigma : \beta\sigma = \hat{V} - \tfrac{1}{2}\hat{U}\hat{X}^{\rm s}\hat{U} - \tfrac{1}{2}(\hat{U} + 2\hat{V})\hat{X}^{\rm c}(\hat{U} + 2\hat{V}). \tag{15}$$

3. SC state in the metallic CO state and the normal state

We analyze the electronic state on the basis of the MF Hamiltonian and examine the SC state with a singlet pairing. The numerical calculation is performed using eV as the units of energy and temperature and kbar as that of pressure, and taking the lattice constant as unity.

Figure 2 shows the pressure dependence of the electron number $n_\alpha = n_{\alpha\uparrow} + n_{\alpha\downarrow}$ and the magnetic moment $m_\alpha = n_{\alpha\uparrow} - n_{\alpha\downarrow}$ at $T = 0.05$, where $\alpha = 1, 2, 3$ and 4 in the extended unit cell of the superlattice due to CO. The insulating state with CO is obtained for $P < 3$ kbar (COI), where the hole-rich sites (1, 4) align along p–q direction and have staggered moments. The electron-rich sites (2, 3), on the other hand, have small magnetic moments. For $3 < P < 4.4$ kbar (COM), the intermediate metallic state is obtained, where the weakened CO still exists but there is no magnetic moment. For $P > 4.4$ kbar, one finds the normal metallic state where both charge density and spin density are uniform. The COI and COM states exhibit a superlattice in which the lattice constant is double along the a-axis. Then the one-dimensional-like Fermi surface is folded and is broken into the electron and hole pockets in the COM state (as shown later). The density of states of the COM state is, however, nearly equal to that of the normal state.

Figure 3 shows the pressure–temperature phase diagram, which consists of COI, COM and normal states. The intermediate state (COM) exists in both the high temperature region and the high pressure region. The inset of figure 3 shows the relative free energies of the COI, COM and normal states, showing the first-order phase transitions among these three states. The COI and normal states coexist as metastable states in the COM state at the intermediate region, since their free energies are located within a narrow energy range of 10^{-3} eV. Moreover the metastable COM state exists in the normal state at higher pressures where the energy difference is within 2×10^{-4} eV. This suggests that these metastable states exhibit phase separation or dynamical fluctuation at finite temperature. Thus the hysteresis may be expected when the CO state emerges or disappears in β''-$(DODHT)_2PF_6$ salt.

In the intermediate region with the COM state, the spin fluctuation is strongly enhanced, while the charge fluctuation is suppressed due to CO. The spin fluctuation exhibits a staggered pattern on sites 1 and 4 corresponding to the characteristic momentum $\mathbf{q}^* = (\pi, \pi)$, i.e. $\chi^{\rm s}_{14}(\mathbf{q}^*) < 0$. Enhancement of the staggered spin fluctuation in the presence of CO has been reported for α-$(BEDT\text{-}TTF)_2I_3$ [10]. It is not due to the enhancement of the density of states or the nesting, but is due to the spin–spin correlation among the self-doped hole-rich

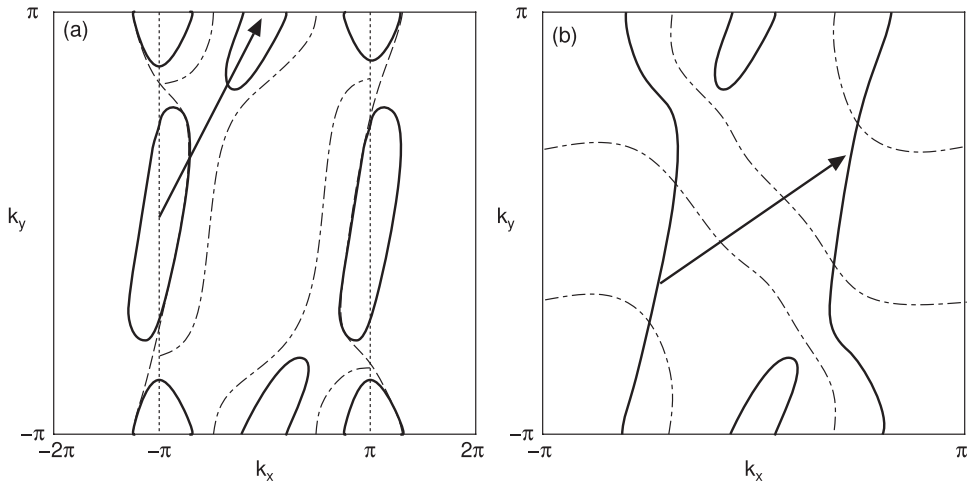

Figure 4. (a) The node line of the SC state in the COM state is shown by the dot–dashed line, where the dotted lines denote the folded Brillouin zone due to the superlattice of the CO. The one-dimensional-like Fermi lines (dashed lines) are broken into electron pockets (the solid line in the middle) and hole pockets (the solid line divided) by the folding. The hole pocket indicated by the solid arrow is not affected by the folding. The solid arrow indicates the staggered spin fluctuation with a characteristic momentum $\mathbf{q}^* = (\pi, \pi)$. (b) The node line of the SC state in the normal state is shown by the dot–dashed line. The one-dimensional-like Fermi lines and the hole pocket are shown by solid lines. The solid arrow represents the charge fluctuation with a characteristic momentum $\mathbf{q}^* = (0.8\pi, 0.6\pi)$.

sites in the CO. The weakened CO with no magnetic ordering induces large spin fluctuation.

For both the COM state and the normal state, we investigate the order parameters and the eigenvalues of the SC states by using the linearized gap equations (8) and (9), which correspond to the singlet SC state and the triplet SC state, respectively. In the present study, the eigenvalues of the triplet SC states are smaller than those of the singlet SC states, e.g. the ratio is about 0.1 within the present choice of our calculation. Therefore we focus on the singlet SC state hereafter.

Now we examine the SC state for the COM. The main component of the anomalous self-energy of the SC state in the intermediate COM state comes from sites 1 and 4, and has momentum dependence given by $\Sigma^a_{14}(\mathbf{k}) \propto \cos(k_x - k_y) +$ const. As shown in figure 4(a), the SC state has node lines (the dot–dashed line) which do not cross the Fermi line (the solid line) in the folded Brillouin zone. The pairing is induced by the staggered spin fluctuation with $\mathbf{q}^* = (\pi, \pi)$ on sites 1 and 4, $\chi^s_{14}(\mathbf{q}^*)$, which connects the electron pocket to the hole pocket (see the solid arrow in figure 4(a)). The Fermi line avoiding the node leads to the gain of the pairing energy. Thus the d-wave SC state with a full gap becomes favorable for pairing, as was pointed out by Kuroki and Arita [21].

In the normal state, the superconductivity mediated by the charge fluctuation can overcome that mediated by the spin fluctuation when the value of the nearest-neighbor interaction becomes close to that of the on-site interaction. In the present case with $U = 0.5$, $V_b = 0.45$ and $V_c = 0.2$, the superconductivity mediated by the charge fluctuation occurs in the normal state near the CO phase. As shown in figure 4(b), there are node lines (the dot–dashed line) which cross the large one-dimensional-like Fermi line (the solid line) four times. The pairing is induced by the incommensurate charge fluctuation with $\mathbf{q}^* = (0.8\pi, 0.6\pi)$ which is determined by the momentum dependences of both the irreducible susceptibility

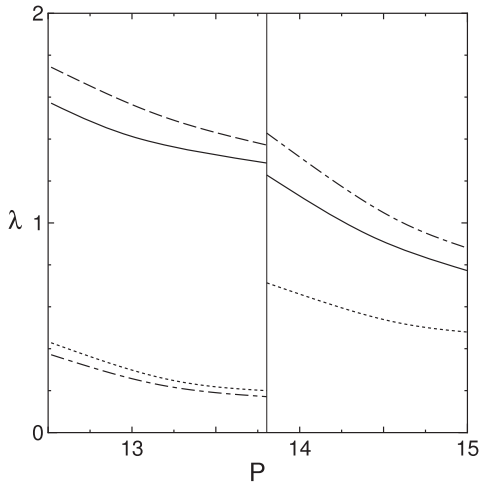

Figure 5. Pressure dependences of the eigenvalues λ of the gap equation (equation (5)) due to the spin fluctuation (the solid line: $V_b = 0.3$ and the dashed line: $V_b = 0.45$) and the charge fluctuation (the dotted line: $V_b = 0.3$ and the dot–dashed line: $V_b = 0.45$) at $T = 0.01$.

(equation (7)) and the nearest-neighbor interactions. This charge fluctuation is given by the arrow in figures 4(b), which connects the one-dimensional-like Fermi lines. We emphasize that the superconductivity in the normal state is the gapless d-wave state, although that in the COM state is the full-gap d-wave state.

Figure 5 shows the pressure dependences of the eigenvalues λ of the gap equation (equation (9)) due to the spin-fluctuation part P^s and the charge-fluctuation part P^c of the pairing interaction at $V_b = 0.3$ and $V_b = 0.45$. Since the charge ordering enhances the spin fluctuation the eigenvalue due to the spin fluctuation is enhanced by V_b in the COM state ($P < 13.8$ kbar), where the solid line is λ for $V_b = 0.3$ and

the dashed line is that for $V_b = 0.45$. In the normal state ($P > 13.8$ kbar), λ of the spin fluctuation is independent of V_b. The eigenvalue due to the charge fluctuation (the dotted line: $V_b = 0.3$ and the dot–dashed line: $V_b = 0.45$) is enhanced by V_b in the normal state, while it is slightly suppressed in the COM state.

4. Discussion

We have investigated the unique electronic states for the CO and SC states described above by applying the mean-field theory and the random phase approximation to the extended Hubbard model. The transfer integrals are given by the extended Hückel calculation using data from x-ray experiments in order to understand the actual electronic state of β''-(DODHT)$_2$PF$_6$ salt. We found the intermediate metallic phase with weakened CO (the COM phase) between the insulating phase with the stripe CO (the COI phase) and the normal metallic phase. There are metastable states in the region close to the intermediate metallic phase of the COM. For example, both the COI state and the normal metal are metastable states in the COM phase. These metastable states have free energies with less than 10^{-3} eV above the free energy of the COM. Then either a phase separation or dynamical fluctuation effects would be expected to occur, which may be relevant to the hysteresis and non-ohmic transport [24]. The spin fluctuation enhanced in the COM state induces superconductivity with the full gap. Such full gap superconductivity where the node line is located between the Fermi pockets is favorable for a pairing mechanism [21]. It was shown in the present paper that the folding of the quasi-1D Fermi surface in the COM state realizes full gap superconductivity. We note that SC in the COM state is similar to that of α-(BEDT-TTF)$_2$I$_3$, i.e. SC in the presence of the stripe CO [10]. The weakened stripe CO under pressure can be a common stage for the SC state in a two-dimensional quarter-filled system. The d-wave superconductivity mediated by the charge fluctuation occurs in the normal state when the nearest-neighbor interaction is as large as the on-site interaction. Such a charge fluctuation is due to nesting on the quasi-1D Fermi surface. Then it connects to the origin of the superconductivity in the vicinity of the charge density wave in α-(BEDT-TTF)$_2$NH$_4$Hg(SCN)$_4$ [20].

Acknowledgments

This work has been financially supported by a Grant-in-Aid for Special Coordination Funds for Promoting Science and Technology (SCF) from the Ministry of Education, Culture, Sports, Science and Technology in Japan, and for Scientific Research on Priority Areas of Molecular Conductors (No. 15073213) from the Ministry of Education, Culture, Sports, Science and Technology in Japan.

References

[1] Ishiguro T, Yamaji K and Saito G 1998 *Organic Superconductors* 2nd edn (Berlin: Springer)
[2] Mori H 2006 *J. Phys. Soc. Japan* **75** 051003
[3] Nishikawa H, Morimoto T, Kodama T, Ikemoto I, Kikuchi K, Yamada J, Yoshino H and Murata K 2002 *J. Am. Chem. Soc.* **124** 730
[4] Yamada J 2004 *J. Mater. Chem.* **14** 2951
[5] Nishikawa H, Sato Y, Kikuchi K, Kodama T, Ikemoto I, Yamada J, Oshio H, Kondo R and Kagoshima S 2005 *Phys. Rev.* B **72** 052510
[6] Kino H and Fukuyama H 1995 *J. Phys. Soc. Japan* **64** 4523
[7] Seo H 2000 *J. Phys. Soc. Japan* **69** 805
[8] Hotta C 2003 *J. Phys. Soc. Japan* **72** 840
[9] Seo H, Hotta C and Fukuyama H 2004 *Chem. Rev.* **104** 5005
[10] Kobayashi A, Katayama S and Suzumura Y 2005 *J. Phys. Soc. Japan* **74** 2897
[11] Tajima N, Ebina-Tajima A, Tamura M, Nishio Y and Kajita K 2002 *J. Phys. Soc. Japan* **71** 1832
[12] Merino J 2007 *Phys. Rev. Lett.* **99** 036404
[13] Watanabe H and Ogata M 2006 *J. Phys. Soc. Japan* **75** 063702
[14] Scalapino D J, Loh E Jr and Hirsch J E 1987 *Phys. Rev.* B **35** 6694
[15] Merino J and McKenzie Ross H 2001 *Phys. Rev. Lett.* **87** 237002
[16] Kobayashi A, Tanaka Y, Ogata M and Suzumura Y 2004 *J. Phys. Soc. Japan* **73** 1115
[17] Tanaka Y, Yanase Y and Ogata M 2004 *J. Phys. Soc. Japan* **73** 2053
[18] Onari S, Arita R, Kuroki K and Aoki H 2004 *Phys. Rev.* B **70** 094523
[19] Tanaka Y and Kuroki K 2004 *Phys. Rev.* B **70** 060502
[20] Nonoyama Y, Kobayashi A and Suzumura Y 2007 *J. Phys. Soc. Japan* **76** 014703
[21] Kuroki K and Arita R 2001 *Phys. Rev.* B **64** 024501
[22] Higa M, Kondo R, Kagoshima S and Nishikawa H 2007 *J. Phys. Soc. Japan* **76** 034709
[23] Kobayashi A, Katayama S, Noguchi K and Suzumura Y 2004 *J. Phys. Soc. Japan* **73** 3135
[24] Kondo R, Higa M and Kagoshima S 2007 *J. Phys. Soc. Japan* **76** 033703